

# Characterization of a Constant Air Volume (CAV) Box Based on Measurements

Zakarya Kabbara <sup>a</sup>, Sandy Jorens <sup>a</sup>, Bert Belmans <sup>b</sup>, Ivan Verhaert <sup>a</sup>.

<sup>a</sup> Faculty of Applied Engineering, Department of Electromechanics, University of Antwerp, Belgium, Zakarya.kabbara@uantwerpen.be

<sup>b</sup> Faculty of Applied Engineering, Department of Civil Engineering Technology, University of Antwerp, Belgium

**Abstract.** HVAC engineers are frequently challenged to design and operate ventilation systems with a high standard of performance considering comfort, energy efficiency, and indoor air quality. However, currently, most design, commissioning and control processes of ventilation systems rely on rules of thumb and engineers' experience. A simulation-based framework for informed decision-making could be an effective tool to achieve ventilation systems with optimal design and performance. To develop such a framework, the integration of solid component models that provide insight into the system's aerodynamic behavior is vital. In previous research, a simulation framework known as Air Distribution Network Design (ADND) optimization algorithm was developed. The ADND algorithm provides a basic strategy to design centralized air distribution networks. However, the method is missing some features before it can be used in practice. Currently, the method is limited to generating layout by accounting for the ductwork only. Some ventilation system components (e.g., CAV control box) are not yet integrated. This paper presents the development of a new CAV control box model that is typically used in nonresidential buildings, viz., a mechanically controlled damper that maintains airflow to a predefined fixed airflow level. The model aims to predict the aerodynamic performance of the control box at any given inlet volumetric flow rate and set airflow rate (i.e., the airflow index at which the CAV box is commissioned to maintain the flow) for diameters between 125 and 250 mm. First, lab setups were built to measure pressure drops for different CAV diameters by varying the inlet airflow rates and set airflow rates. Next, the measurement data was used to develop a model of the CAV control box by training a regression model. Finally, the model was tested and validated on experimental data that was not used in the training set. The accuracy of the CAV box model justifies its integration into the ADND algorithm and also its potential to be integrated into common building simulation frameworks. Once integrated, it can be exploited in many applications, including evaluating the performance of designs, automating the iterative balancing process, and optimizing the control strategy of ventilation systems.

**Keywords.** Mechanical Ventilation, Constant Air Volume (CAV) box, CAV systems, Simulation Framework, Design optimization

**DOI:** <https://doi.org/10.34641/clima.2022.157>

## 1. Introduction

### 1.1 Overview

Nowadays, HVAC engineers are challenged to design and operate ventilation systems with a high standard of performance concerning comfort, energy efficiency and indoor air quality (IAQ) at minimal expenses (i.e., material, installation and maintenance costs). However, most of these features contradict; for example, achieving the desired IAQ, i.e., CO<sub>2</sub> levels, is usually reached by increasing the supply and/or extract airflow rates, which concurrently increases the energy usage and sound levels. This illustrates that achieving an optimal design and

system operation can be complex. Consequently, design and operation decisions still often rely on rules of thumb [1,2]. Therefore, a method supporting and guiding engineers in designing, commissioning, and controlling ventilation systems would be desirable.

Previous research developed an optimization method for Air Distribution Network Design (ADND) [1,3]. This method can quickly generate numerous different air distribution system configurations (i.e., ductwork layout and duct sizes). The method provides a basic strategy to generate optimized air distribution network designs for nonresidential buildings. Although the ADND optimization method

results in promising outcomes, some additional features are required before it can be used in practice. Currently, the method is limited to generating layouts by accounting for ductwork only. Ventilation system components (i.e., diffusers, silencers and volume flow controllers) are not yet included in the ADND method [1,2]. Implementing all existing ventilation components to the ADND algorithm devotes the potential for further design optimization.

To integrate the missing components in the ADND algorithm, it is essential to have aerodynamic models for every component that may exist in the ductwork. These component models should predict the pressure drop as a function of airflow rate by allowing input for all the parameters that may affect the aerodynamic performance of the component (e.g., inlet and outlet dimensions in case of a transition or bend angle in case of a bend). Most of these component models exist in literature, design standards, building simulation frameworks or are provided by the manufacturer [4,5]. However, some component models solely exist at a high abstraction level, while others do not exist at all. Therefore, they cannot be integrated into the ADND optimization algorithm as they cause performance inaccuracies. One of these components is the Constant Air Volume (CAV) box.

Several CAV box types are used in practice. Some of them are inserted inside the ducts Fig 1-B. These types of CAV boxes are often used in residential buildings as they are only suitable for low velocities and small sizes. However, the ADND algorithm is still limited to designing air distribution systems in nonresidential buildings. The CAV box that is typically used in nonresidential buildings is the one having a blade and control mechanism presented in Figs 1-A and 1-E. It is inserted at both sides into a round duct for easier installation and maintenance. This CAV box can have several control settings depending on the manufacturer (Figs 1-C and 1-D), but always the same controller structure and function (i.e., blade type and spring connection). This paper focuses on developing a CAV box that is often used in nonresidential buildings.

### 1.2 CAV Mechanism

A CAV control box ideally maintains the passing volumetric flow rate at a predefined fixed level, independently of the pressure variation upstream or downstream in the air distribution network. In practice, this can be achieved to a certain extent by respecting the minimum and maximum pressure difference over the CAV box. The CAV box is a mechanically self-powered unit that controls airflow by setting an external controller assembly mounted on the CAV (Fig 1-C-D). The control assembly provides an index for the range of airflow rates (i.e., Qsets) that the CAV box can maintain to achieve the demand flow. The desired flow rate is usually set while commissioning the air distribution system.

In a random hydraulic component, the flow rate is directly proportional to the square root of the pressure drop. Thus, the flow rate increases with the pressure drop and vice versa. To achieve a fixed flow rate for a range of pressure variations over the inlet and outlet of the CAV box, the blade inside the CAV box should close when the inlet pressure is high and vice versa. This is achieved by the blade shape presented in Fig 1-F. Due to the bend shape of the blade, the blade is dragged to a more closed position at higher inlet pressure, reducing the opening area and flow rate. A spring provides a counterforce to regulate the opening position according to certain inlet pressure. At lower pressures, the spring pushes the blade back to a more open position.

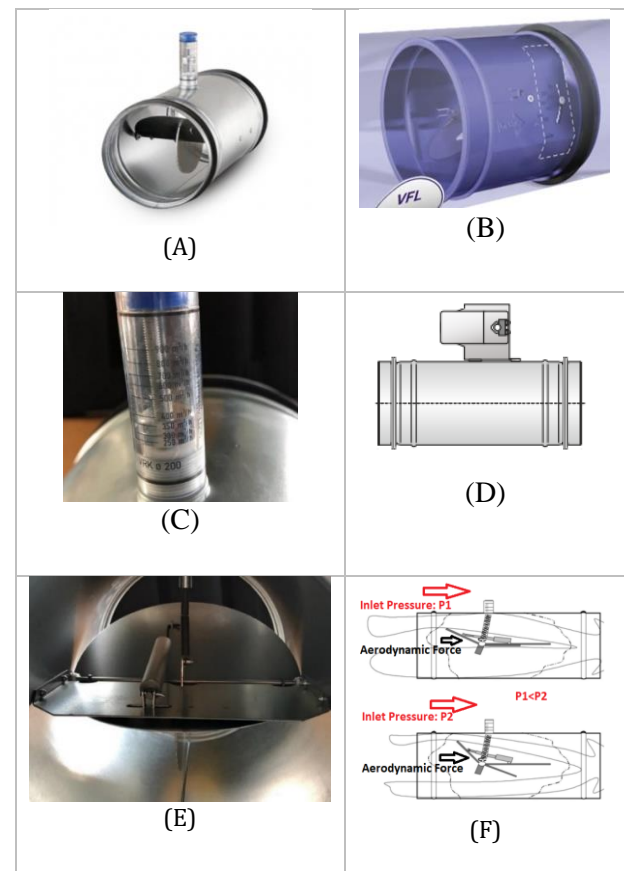


**Fig. 1 - :** (A): Nonresidential CAV box (B): Residential CAV box (C-D): Two different CAV Controller Assemblies (E): CAV blade with a spring attached; (F): Aerodynamic force sketch [6].

Considering physical limitations, in general, the CAV has three working areas. At low inlet pressure, the CAV is almost fully open, and the flow rate is directly linked to the available pressure drop. At very high inlet pressure (typically beyond the operational limit), uncertain behavior of the airflow vs. the pressure drop occur due to the developed vortices (more explanation in section 3.2). In between these limits, the maintaining phase occurs where the airflow rate is ideally fixed.

### 1.3 State of the Art

Some ventilation components' manufacturers

provide the CAV box's aerualic curve models (i.e., airflow rate vs pressure drop curve) [7]. However, those curves describe the CAV box's performance only when the box is operating at the maintaining phase. Nevertheless, the transition phase (the phase at low-pressure drops before the maintaining phase) is not included in the curves. Furthermore, the curves are averaged for several diameters for every Qset. This leads to imprecisions when determining which pressure drop is required to maintain a particular airflow rate (Fig 2). The imprecisions of averaging the curves were proven by experimental measurement (graphically presented in sections 2 and 3); while changing the diameter of the CAV box and commissioning it at the same Qset, the pressure required to maintain the airflow rate is different for every diameter. For example, considering a Qset=250 m<sup>3</sup>/h, the airflow is maintained for a CAV box diameter of 160mm when the pressure drop is 50 Pa. On the other hand, for a diameter of 200mm, the airflow is not maintained until reaching a pressure drop of 75 Pa. Consequently, this will affect the aerualic performance assessment of the ADND algorithm and, therefore, the design decisions.

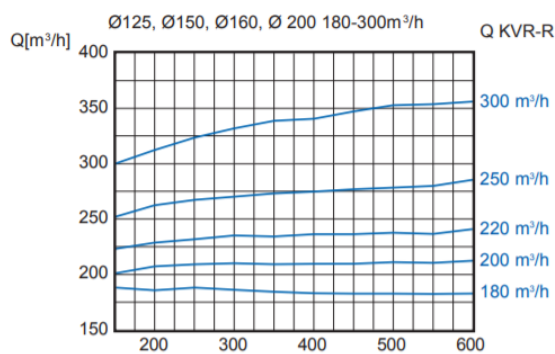


**Fig. 2** - Airflow rate vs pressure drops for diameters 125, 150, 160, 200 and airflows between 180 and 300 m<sup>3</sup>/h [7].

CAV boxes are often used in CAV ventilation systems, where the system supplies a constant airflow rate at variable temperatures [8]. Therefore, a CAV damper that maintains the airflow at a specified airflow rate is implemented in common building simulation frameworks (i.e., EnergyPlus [9]). However, the damper models do not allow to exceed their maximum set airflow rate (i.e., Qset) [9]. Ideally, this is how CAV boxes are meant to perform. Therefore, the common simulation frameworks assume ideal CAV box performance. However, manufacturers declare that there might be an airflow rate deviation of  $\pm 10\%$  in the stable control range (i.e., maintenance range) [10,11].

Furthermore, CAV boxes can also operate with partial load behavior in practice. For example, during the daytime, the building is fully occupied; thus, the system operates at full load; nevertheless, at night, the building is almost unoccupied; thus, the system operates at partial load. Such a system is still a CAV system with two operating modes (i.e., day and night modes). Moreover, CAV boxes are also used in variable air volume (VAV) systems, where partial

airflow behavior or demand-controlled ventilation occurs (i.e., Building Z – UAntwerpen, Belgium). In the same VAV air distribution system, there might be rooms with a VAV box as a volume flow controller and other rooms with a CAV box volume flow controller. For example, considering a VAV system, VAV boxes (i.e., automatically adjusted dampers) are installed to control the airflow in rooms with unstable occupancy behavior (e.g., meeting rooms) by controlling the damper position and the AHU fan. On the other hand, the CAV boxes are installed in the system for rooms with a stable demand profile (i.e., storage rooms), as they are much cheaper than the VAV boxes. Nonetheless, the CAV box model developed in the common simulation framework cannot operate in partial load behavior or a VAV system. For instance, in EnergyPlus, the CAV box, which is categorized under the terminal components (i.e.,

Air:Terminal:SingleDuct:ConstantVolume:NoReheat), is not allowed to be implemented in a system with a variable airflow fan [9]. However, an alternative for a CAV box in a VAV system used by design developers is a VAV box with a constant flow control signal to maintain the airflow rate. Although the alternative is meant to control airflow rate, it does not have the same aerualic performance because CAV and VAV boxes have different mechanisms. Therefore, integrating the CAV box model of the common simulation frameworks or its alternative during partial load behavior in the ADND algorithm leads to an inaccurate aerualic performance and defect in the design optimization potentials. The desired CAV model to be integrated into the ADND algorithm should estimate the aerualic performance (i.e., pressure drop vs. airflow rate) for all available sizes and Qsets within the operational limit, i.e., low-pressure phase and intermediate pressure phase or maintaining phase.

#### 1.4 Aims and Objectives

Since no CAV box model is compatible with the ADND algorithm, a CAV box model that can mimic the aerualic performance of a real CAV box is needed mainly to be integrated into the ADND algorithm for further optimization. This model will also be useful for integration into common simulation frameworks to make better aerualic performance predictions than with existing models.

In this paper, a model for the CAV box that is typically used in nonresidential buildings is developed to determine its aerualic performance for any given Qset of the CAV box diameters between 125 and 250mm. Lab setups for three CAV boxes with three different diameters (i.e., 125, 160, and 200 mm) were constructed at the HVAC Lab – University of Antwerp. First, pressure drop and airflow rate measurements were collected, as discussed in section 2.1. Next, airflow rate vs. total pressure drop curves for the three CAV boxes at every airflow rate index (i.e., Qset) were fitted to the collected measurements, as discussed in section 2.2. Curves fitting was only applied to the collected measurements for the three

tested diameters (results are presented in section 3.1). However, it allowed the generation of enough data to train an artificial neural network (ANN) regression model that can predict the aerualic performance (i.e., total pressure drop vs. airflow rate and vice versa) of any existing CAV box with a particular diameter and Qset range. An ANN regression model was used due to uncertainty on the CAV box aerualic performance. Simply interpolating and extrapolating between the fitted curves proved to be less accurate than the ANN predictions, especially when extrapolating to a CAV box with a different diameter. Further explanation of why ANN was the chosen approach to develop the CAV model is presented in section 3.2. The results, validation, and discussion on the application potential are included in section 3.3.

## 2. Methodology





### 2.1 Experimental Measurements

The American Society of Heating, Refrigerating and Air-Conditioning (ASHRAE) standard [12] is used to measure the pressure drop of the CAV box and the volumetric flow rate in the branch with the CAV box. The performed setups for the three CAV box diameters follow the description of duct mounted fitting test setup [12,13] where,

- The distance before the fitting is at least 4.6m to achieve a fully developed flow. For the CAV setups, the distance before the CAV box was at least 6 m.
- The total pressure drop is measured at a distance of  $(1.5 \pm 0.5)D$  upstream (i.e., before the CAV box) and  $11D$  downstream (i.e., after the CAV box), where  $D = \text{diamter of the inlet duct} = \text{diamter of the outlet duct}$ . The pressure difference upstream and downstream is the sum of the total pressure drops from the CAV box and the duct parts between the upstream and downstream measuring points.
- The air velocity measurement plane is at least 7.5 diameters downstream. Fig 3 represents the measurements locations per diameter. A volume flow hood was placed at the terminal of each test setup to ensure the velocity measurements. Therefore, the velocity and the airflow rate measurements are expected to match.

The measuring instruments and their accuracy are presented in Tab. 1.

Tab. 1- List of Instruments

Type-of measurements	Instrument	Error	Serial Number
Multi-function measuring instrument, which was used for pressure and velocity measurements		$\pm (0.3\text{Pa} + 1\%)$	0563 4800
Pressure		Follows the multi-function measuring instrument	0635 2045
Velocity		$\pm (0.2\text{m/s} + 1\%)$	0635 9542
Volume flow rate		$\pm 3\%$	0563 4200

### 2.2 Data Augmentation

Experimental setups were created on three CAV boxes with 125, 160, and 200mm diameters to develop an empirical CAV model that can predict its aerualic performance at any given diameter and Qset. For each diameter, 7 to 8 Qsets were tested. For each Qset, at least eight airflow rates and total pressure drop measurements must be taken, according to ANSI/ASHRAE standard 120-2017 [12].

After measuring the data, one way to develop the CAV model would be by interpolating and extrapolating the available measured data to determine the aerualic performance at any given diameter and Qset. Several input parameters may affect the aerualic performance of the CAV box (i.e., airflow rate, pressure, diameter, Qset). Interpolation and extrapolation can be performed to estimate the aerualic performance by following the existing trend of measured data. Interpolation and extrapolation can only be valid to know the aerualic performance between two measured points having the same diameter and Qset. However, interpolating and/or extrapolation between points having different diameters and/or Qsets results in an inaccurate output due to the CAV box uncertainty in the aerualic performance. For example, the CAV box of 200mm with Qset= 300 m<sup>3</sup>/h had eight measured points (airflow vs. pressure drop); interpolating between



the eight measured points to determine the airflow vs. the pressure drop can give an accurate result. However, extrapolating to an unmeasured diameter (i.e., 250mm) to determine aeraulic performance results in inaccurate outputs due to the CAV box uncertainty. Section 3.2 presents the CAV box's aeraulic performance uncertainties and justifies why interpolating and extrapolating between the measured data is inaccurate. To overcome the uncertainties, curves are first fitted to the measured data to generate enough data to train a regression model. The fitted curves are shown in Figs 4, 5, and 6. An accurate correlation that can describe the equation of the measured data is equation 1.

$$Q = A + (B \times PD) - C e^{-D \times PD} \quad \text{Equation 1}$$

Where Q is the airflow rate [m<sup>3</sup>/h], PD is the pressure drop [Pa], A, B, C, and D are coefficients that are estimated for each curve using the `curve_fit` function from the SciPy library on Python [14]. The R squared value for every fit is estimated to indicate how well the curve fits the measured data. The closer the R squared value to 1, the more accurately the curve is fitted to the data. Although the R squared function can also be imported from the scikit-learn library [15] in Python, its correlation is presented in equation 2.

$$R^2 = \frac{\Delta_{mean} - \Delta_{fitted\ curve}}{\Delta_{mean}} \quad \text{Equation 2}$$

Where  $\Delta_{mean}$  is the variation around the mean, which is the sum of the square differences between the actual measured values and the mean.  $\Delta_{fitted\ curve}$  is the sum of the square differences between the actual measured value and the predicted ones from the fitted curve.

After fitting the curves to the measured data, enough data can be generated by implementing parameters into equation 1. The generated data is used to train an ANN model to predict the aeraulic performance of the CAV box, given its diameter and Qset. The model prediction is expected to be accurate even when inputting different diameters (e.g., 250mm) and Qsets than those used for training. The diameters and Qsets that were used for training are presented in Table 2.

### 2.3 The ANN Model

ANN has been an attractive tool for solving nonlinear problems [16], making it suitable to describe the nonlinear performance of the CAV box. ANN learns from the data provided, i.e., training dataset. The training dataset for the CAV box model is the measured data (section 2.1) and the expanded data (section 2.2). The input parameters for training the ANN regression model are the diameter of the CAV box, Qset, and the total pressure drop. The output of the model is the airflow rate. Besides, ANN can deal with uncertainties, which are discussed in section 3.2.

## 3. Results

This section presents the outcomes of the curve fitting of the measured data in section 3.1. Then, the fitted curves are used to generate more data (as discussed in section 2.2) to train an ANN regression model, i.e., the CAV box model that predicts the aeraulic performance given at any given diameter and the Qset of the intended CAV box. Before reporting the model results, some measurement observations and the reason for using the ANN regression model is used are presented in section 3.2. Finally, the trained CAV model results and the model validation are presented in section 3.3.



Fig. 3 - Experimental setup – UAntwerpen HVAC Lab

### 3.1 Curve Fitting

The minimum and maximum R squared of the fitted curves are presented in table 2.

**Tab. 2** - R squared outputs for the fitted curves

CAV Diameter (mm)	Qset [m <sup>3</sup> /h]	R squared
125	125, 150, 175, 200, 225, 250, 280	Min = 0.9926 Max = 0.9989
160	180, 200, 250, 300, 350, 450, 500	Min = 0.9935 Max = 0.9996
200	250, 300, 350, 400, 500, 600, 700, 800	Min = 0.9889 Max = 0.9996

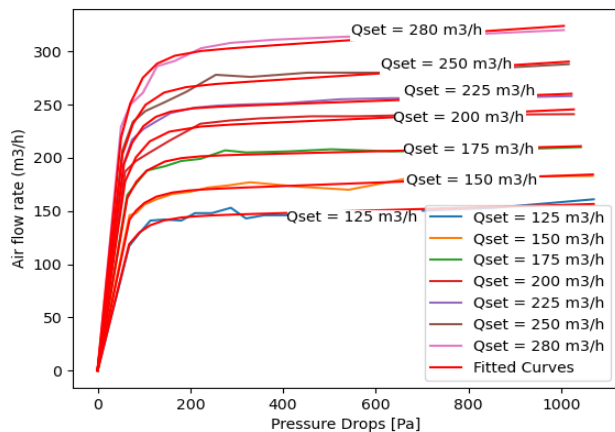


**Fig. 4** - Airflow rate vs total pressure drop for 125 mm CAV box

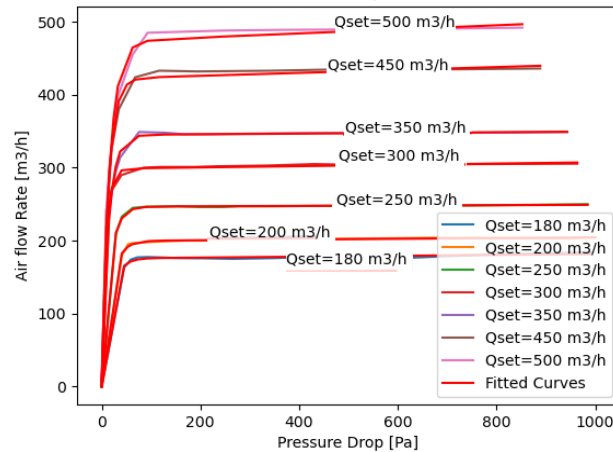


**Fig. 5** - Airflow rate vs total pressure drop for 160mm CAV box

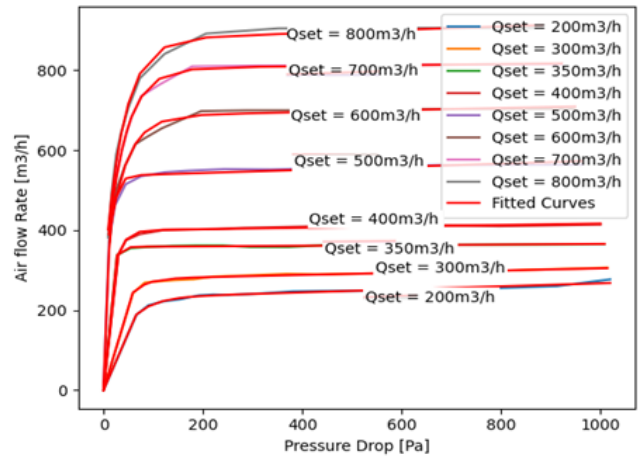


**Fig. 6** - Airflow rate vs total pressure drop for 200mm CAV Box

From the fitted curves, 2100 data sets (i.e., Pressure Drop, CAV diameter, Qset, actual airflow rate) were generated to train an artificial neural network (ANN) regression model that predicts the airflow rate given the pressure drop at any given CAV diameter and its Qset.

### 3.2 Curves Behaviour

From Figs 4, 5, and 6, it can be observed that to reach the constant airflow rate; the fan must supply enough pressure to overcome the first part of the curve, i.e., where the pressure drop from the CAV box is usually between 0 and approximately 75 Pa. The second part of the curve is where the CAV is desired to function, i.e., where the airflow rate barely changes with the increase of the fan pressure. In this latter part, the CAV blade closes to drop enough pressure, thus maintaining the airflow rate. The last part of the curves is presented in Fig 7. Although this region is reached at a high-pressure inlet of the CAV box (>600 Pa), in practice, this part is unlikely to be reached as it requires too much power from the fan and produces too much noise along the ductwork. Besides, the pressure in this part of the curve is often higher than the operating range of the CAV box. The high inlet pressure results in unstable behavior of the curve, where the airflow rate starts to fluctuate around the stable airflow rate. The fluctuation is due to the vortices developed after the CAV box. These vortices can result in forces opposite or the same counterforce direction discussed in section 1.2. Therefore, these vortices can help open or close the CAV blade, leading to an increase or decrease in the airflow rate. However, while fitting the curves, the average airflow of these fluctuations is considered.

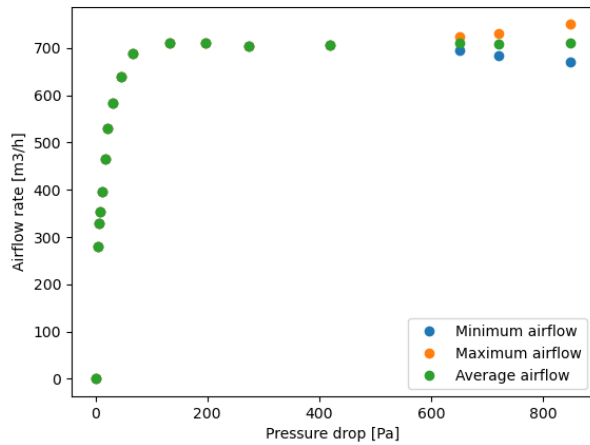


**Fig. 7** - Airflow rate vs. total pressure drop for 200mm CAV box ( $Q_{set} = 600 \text{ m}^3/\text{h}$ )

Although  $Q_{set}$  is the index where the airflow rate is supposed to be maintained, it can be observed from Figs 4, 5, and 6 that in most of the curves, the airflow rates are maintained at a slightly different airflow. For example, in Fig 6, when  $Q_{set} = 600 \text{ m}^3/\text{h}$ , the airflow rate is not maintained until around  $650 \text{ m}^3/\text{h}$ . The manufacturers declare that this difference in airflow rate can arise in the maintaining range, and it is often quantified as 10% airflow control accuracy [10,11]. This means that in order to maintain the airflow rate at  $600 \text{ m}^3/\text{h}$ , the airflow index should be commissioned somewhere between  $Q_{set} = 500 \text{ m}^3/\text{h}$  and  $Q_{set} = 600 \text{ m}^3/\text{h}$ .

For a CAV box model, which can predict the aerualic performance at any given CAV box diameter and its  $Q_{set}$ , interpolation and extrapolation are inaccurate techniques in predicting the aerualic performance. This is due to the uncertainties of the CAV aerualic performance. To be more specific, typically,  $Q_{set}$  is the index where the airflow is maintained. By observing Fig 4, where the diameter of the CAV box is 125mm, the airflows are maintained at a value slightly higher than their  $Q_{sets}$ . On the other hand, for a CAV box diameter of 160mm, the airflows are maintained at a slightly lower value than their  $Q_{sets}$  (Fig 5). By extrapolating between these 125mm and 160mm to predict the aerualic performance of a 200mm CAV box, the airflow rates are expected to be maintained at a lower value than their  $Q_{sets}$ . However, the measured data proved that this is not the case. From Fig 5, it can be observed that the measured airflow rates are most of the times maintained at a value slightly higher than the  $Q_{set}$  (i.e.,  $Q_{sets} = 350, 400, 500, 600, 700, \text{ and } 800 \text{ m}^3/\text{h}$ ) but maintained once at an airflow rate lower than the  $Q_{set}$  (i.e.,  $Q_{set} = 300 \text{ m}^3/\text{h}$ ). Since ANN learns from the training dataset without requiring prior knowledge of the relationships between process parameters [16], it is expected to deal with the uncertainties properly. Furthermore, the collected measurements proved that the  $Q_{set}$  is just an index to demonstrate a roughly maintained airflow rate. However, by commissioning the same  $Q_{set}$  on different diameters, the airflows are not maintained

at the same airflow. For example, considering  $Q_{set} = 350 \text{ m}^3/\text{h}$  for CAV box diameter of 160 and 200mm (Figs 5 and 6), the airflows are maintained at  $330 \text{ m}^3/\text{h}$  and  $375 \text{ m}^3/\text{h}$ , respectively. Although the difference seems to remain small ( $\pm 10\%$  from the  $Q_{set}$ ), it accumulates with several CAV boxes in an air distribution system. This leads to a less energy-efficient system because the CAV boxes are not well commissioned. As the developed model should predict the airflow rate vs. the total pressure drop at any given  $Q_{set}$  and diameter of the CAV box, it is vital to determine the best position to set the index (i.e.,  $Q_{set}$ ), i.e., where the desired airflow is maintained. This will be automated while integrating the CAV model into the ADND algorithm.

### 3.3 The Model

The developed empirical model of the CAV box is a BlackBox model that predicts the aerualic performance (i.e., airflow vs. pressure drop) for any given diameter and  $Q_{set}$  of the CAV considering the chosen CAV type that is typically used in nonresidential buildings. The model trains the data collected from the fitted curves in sections 2.1 and 2.2 on the ANN regression model. The model has four hidden layers with a total of 40 units.

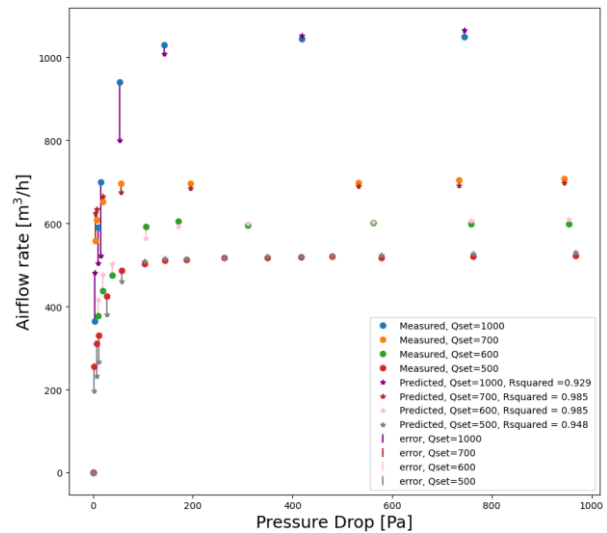


**Fig. 8** - Predicted and measured airflow rate as a function of pressure drop for 250mm CAV box

Two validation methods were undertaken to validate the developed CAV box model. First, while training the model, 20% of the collected dataset was randomly taken to test the outputs of the trained ANN model. The test dataset included data for CAV diameters of 125, 160, and 200mm at different  $Q_{sets}$ . The R squared value of the test set is approximately 0.98.

The other validation method was performed on CAV boxes with diameters that were not included in the training process. Therefore, these CAV boxes' experimental setup was also built by committing to the measurements standard in section 2.2 to collect pressure drop and airflow rate for some of their  $Q_{sets}$ . Fig. 8 represents the measurements and the

predicted outputs from the trained model for the CAV box of 250mm diameter and Qset of 500, 600, 700, and 1000 m<sup>3</sup>/h. It can be observed that the trained model predicts accurate outcomes in the maintaining phase (i.e., accuracy of at least 93%). However, less accuracy occurs in the transition phase (the phase at low-pressure drops before the maintaining phase). This is because the data from the transition phase accounts for less than 10% (0 up to 100 Pa) of the entire range of each curve (0 up to 1000 Pa); the rest of the data (more than 90% of the data) are in the maintaining phase. Still, the prediction accuracy in the transition phase did not fall below 75%.

## 4. Conclusion

To conclude, an empirical CAV box model for typical CAV boxes used in nonresidential buildings was developed using experimental lab measurements. The measured data were fitted into curves. These curves allowed the expansion of the measured data to acquire enough data to train the ANN regression model. The ANN regression model is the CAV empirical model that can mimic the aeraulic performance of the CAV box at any given Qset for diameters between 125 and 250mm. To achieve the model that can mimic the aeraulic performance at any given CAV box diameter, data from experimental measurements for diameters smaller than 125 mm and higher than 250 mm can be included in the ANN training dataset.

The predicted outcomes from the developed model matched the experimental dataset of the CAV control box with an accuracy of at least 75% during the transition phase and 93% during the maintaining phase. Therefore, the model's outcomes endorse integrating it into the ADND algorithm to optimize air distribution systems further (i.e., design, commissioning, and control optimization). Moreover, it can be integrated into the common simulation frameworks, where less accurate CAV box models are used.

## 5. Acknowledgment

This work has been supported by the Flemish Agency for Innovation and Entrepreneurship (VLAIO) in the Flux50 project Smart Ventilation (HBC.2020.2520).

## 6. Reference

[1] Jorens S, Verhaert I, Sørensen K. Design optimization of air distribution systems in non-residential buildings. University of Antwerp; 2021.

[2] Jorens S, Sørensen K, Verhaert I, De Corte A. Air distribution system design optimization in non-residential buildings: Problem formulation and generation of test networks. *J Build Eng* [Internet]. 2017;12(May 2017):60–7. Available from:

<http://dx.doi.org/10.1016/j.jobe.2017.05.006>

[3] Jorens S, Verhaert I, Sørensen K. Design optimization of air distribution systems in non-residential buildings. Vol. 175, *Energy and Buildings*. 2018. 48–56 p.

[4] Smith S. Determination of K-Factors f HVAC system components using measurement and CFD modelling. University of Nottingham; 1998.

[5] ASHRAE. *ASHRAE Handbook of Fundamentals*. Vol. 30329. 2009. 926 p.

[6] Halton RMC. Airflow management damper (CAV) [Internet]. Available from: [https://www.halton.com/products/mechanica-l-cav-damper-rmc-en\\_gb/#:~:text=Constant airflow damper Halton RMC, system balancing is not needed.](https://www.halton.com/products/mechanica-l-cav-damper-rmc-en_gb/#:~:text=Constant airflow damper Halton RMC, system balancing is not needed.)

[7] Cairox. KVR-R • Adjustable constant air volume dampers [Internet]. Available from: <https://www.cairox.be/EN/documentation/BO2.010.1BIS-KVR-R-Adjustable-constant-air-volume-dampers/?cf=721543641184212748f816>

[8] Yan Y, Luh PB, Pattipati KR. Fault diagnosis of HVAC: Air delivery and terminal systems. *IEEE Int Conf Autom Sci Eng*. 2017;2017-Augus(2):882–7.

[9] Engineering Reference; U.S. Department of Energy. EnergyPlus [Internet]. EnergyPlus v.9.6.0; 2021. Available from: <https://energyplus.net/>

[10] Aerotechnik. Volume flow controller [Internet]. Vol. 49. 2019. Available from: [https://www.aerotechnik.de/fileadmin/download/en/prospekte/Best-Nr\\_233.pdf](https://www.aerotechnik.de/fileadmin/download/en/prospekte/Best-Nr_233.pdf)

[11] Trox. CAV controllers Type VFC [Internet]. 2017. Available from: <https://www.trox.de/en/cav-controller/vfc-20c13b1afbcd54d>

[12] ANSI/ASHRAE Standard 120-2017. Method of Testing to Determine Flow Resistance of HVAC Ducts and Fittings. 2017. Atlanta, GA: ASHRAE

[13] ANSI/ASHRAE Standard 41.2-2018. Standard Methods For Air Velocity And Airflow Measurement. 2018.

[14] Virtanen P, Gommers R, Oliphant TE, Haberland M, Reddy T, Walt SJ Van Der, et al. *SciPy 1.0: fundamental algorithms for scientific computing in Python*. 2020;17(March).

[15] Raschka S, Mirjalili V. *Python Machine Learning*. Third Edit. 2019.

[16] Živković Ž, Mihajlović I, Nikolić Đ. Artificial neural network method applied on the nonlinear multivariate problems. *Serbian J Manag*. 2009;4(2):143–55.

## Data Statement

The dataset generated during and/or analyzed during the current study are available in the [data.zip](#) repository.